Crystal Structure and Enzymatic Degradation of Poly(4-hydroxybutyrate)

Fengyu Su,[†] Tadahisa Iwata,*[,†] Fumio Tanaka,[‡] and Yoshiharu Doi[†,§]

Polymer Chemistry Laboratory, RIKEN Institute, 2-1 Hirosawa, Wako-shi, Saitama, 351-0198, Japan, Wood Research Institute, Kyoto University, Uji-shi, Kyoto, 611, Japan, and Department of Innovative and Engineered Materials, Tokyo Institute of Technology, 4259 Nagatsuta, Midori-ku, Yokohama, 226-8502, Japan

Received April 28, 2003; Revised Manuscript Received June 30, 2003

ABSTRACT: The crystal structure of poly(4-hydroxybutyrate) (P(4HB)) has been determined by interpretation of X-ray fiber diagrams of a stretched−annealed film and electron diffraction patterns of lozenge-shaped single crystals prepared from ethanol solution. The unit cell of P(4HB) is orthorhombic with space group $P2_12_12_1$ and parameters $a = 0.775 \pm 0.002$ nm, $b = 0.477 \pm 0.002$ nm, and c (fiber axis) $= 1.199 \pm 0.002$ nm. There are two chains per unit cell, which exist in an antiparallel arrangement. The chain conformation has been analyzed through energy minimization by using the Cerius[2] software. The helical conformation is characterized as a slightly distorted all-trans conformation. Molecular packing of this structure has been studied in detail taking into account both diffraction data and energy calculations. Setting angles, with respect to the b axis, are ±29° for the corner and center chains according to intensity measurements and structure factor calculations. Films and solution-grown lamellar crystals of P(4HB) were enzymatically degraded with lipase from *Pseudomonas* sp. and PHB depolymerase from *Pseudomonas stutzeri* YM1006. The enzymatic degradation of solution-cast, stretched, and stretched−annealed films of P(4HB) with lipase was investigated by means of weight-loss profiles and scanning electron microscopy. Furthermore, the enzymatic degradation of P(4HB) single crystals with lipase and PHB depolymerase was studied by using transmission electron microscopy, atomic force microscopy, and gel permeation chromatography. All the smooth edges of the lozenge-shaped lamellar crystals became rough after enzymatic degradation. In the meanwhile, no obvious changes of molecular weights and lamellar thickness were observed. Therefore, it is concluded that enzymatic degradation of the crystal region progressed from the crystal edges rather than the chain-folded surfaces.

Introduction

Poly(4-hydroxybutyrate) (P(4HB), $[-(CH_2)_3-CO-O-]_n$), which is produced by microorganisms,[1−3] is currently receiving much attention in the medical field because of its physical properties as well as biocompatibility.[4−7] Among aliphatic polyesters of the type $[-(CH_2)_m-CO-O-]_n$, the structures of single crystals have been resolved for poly(β-propiolactone) (PPL),[8] poly(δ-valerolactone) (PVL),[9] and poly(ϵ-caprolactone) (PCL).[10−12] The interesting phenomena are that PPL ($m = 2$) and PVL ($m = 4$) have the all-trans conformation in single crystals, while PCL ($m = 5$) has a 2_1 helix conformation. It seems that the number of methylene groups plays an important role in the conformation; that is, the molecular chain takes an all-trans or a 2_1 helix conformation when m is even or odd, respectively. Considering the number of methylene groups, P(4HB) ($m = 3$) is adjacent with PPL and PVL; therefore, the solution of the molecular and crystal structure of P(4HB) will help us to understand the relationship of molecular conformation with methylene number of aliphatic polyesters.

In the preliminary studies on structural analysis of P(4HB) carried out by Mitomo et al.[13,14] and Pazur et al.,[15] they reported the X-ray fiber diagram of P(4HB) from the necking-stretched and annealed film. The unit cell of P(4HB) is orthorhombic with space group $P2_12_12_1$ and parameters $a = 0.775$ nm, $b = 0.479$ nm, and c (fiber axis) $= 1.194$ nm. As for the conformation of the P(4HB) chain, Mitomo et al.[14] reported that the conformation of the P(4HB) chain is similar to that of PCL. Pazur et al.[15] performed energy calculations on a single chain of P(4HB) and finally found five minimum-energy conformers. Among them, one conformer possessing a pitch of 1.19 nm is in good agreement with the observed fiber diagram pitch. Nakamura et al.[16] have carried out molecular mechanics calculations on a single chain with 15 residues by using the MM2 program, and the optimized chain was near all-trans form. Recently, our group[17] succeeded in obtaining solution-grown single crystals of P(4HB) and reported almost the same unit cell dimensions determined by X-ray fiber diagrams of a stretched−annealed film combined with electron diffraction diagrams of single crystals. However, until now, a detailed analysis of conformation and packing structure has not yet been performed.

In this paper, the conformation and packing analysis of P(4HB) crystals have been studied in detail taking into account both diffraction data and energy calculations by using the Cerius[2] program.

As the most well-known biodegradable polyhydroxyalkanoate, poly([*R*]-3-hydroxybutyrate) (P(3HB)) has been widely investigated concerning its synthesis, crystal structure, and degradation process.[18−23] The biodegradation of P(3HB) was carried out on its films[24−27] and lamellar single crystals.[28−32] The results have showed that the enzymatic degradation of P(3HB) preferentially occurred in the amorphous region and subsequently in the crystalline region of the films, and that for the

* To whom correspondence should be addressed. E-mail: tiwata@postman.riken.go.jp. Tel: +81-48-467-9586. Fax: +81-48-462-4667.
† RIKEN Institute.
‡ Kyoto University.
§ Tokyo Institute of Technology.

10.1021/ma034546s CCC: $25.00
Published on Web 07/31/2003

lamellar single crystals, the degradation took place at the crystal edges rather than the chain-folded surface. The syntheses and enzymatic degradation of P(3HB-*co*-4HB) copolymer are also interesting and have been well studied.[33−37] P(3HB-*co*-4HB) films could be hydrolyzed by both PHA depolymerase and lipase, and the degradation rates depended on the monomer fraction. For example, the degradation rate of the films by lipase increased with an increase in the 4HB fraction,[34] while the P(3HB) homopolymer was not attacked by the lipase.[38]

Compared to P(3HB) and P(3HB-*co*-4HB), the crystal structure and degradation of P(4HB) have not been studied in detail, mainly because of difficulties in producing highly pure samples and preparing well-ordered crystals. Recently, substantial amounts of P(4HB) homopolymer have been produced by genetically engineered bacteria.[37,39] Furthermore, we reported the preparation of stretched films and single crystals using the P(4HB) homopolymer synthesized in a recombinant *Comamonos acidvorans* (JCM 10181).[17,37]

In this paper, we have attempted to elucidate the crystal and molecular structure of P(4HB) and the enzymatic degradation mechanism of P(4HB) films and solution-grown lamellar single crystals by means of X-ray diffraction, scanning electron microscopy (SEM), transmission electron microscopy (TEM), atomic force microscopy (AFM), and gel permeation chromatography (GPC).

Experimental Section

Materials. The bacterial P(4HB) sample used in this study was prepared using a recombinant *C. acidvorans* (JCM 10181).[17,37] The weight-average molecular weight (M_w) and polydispersity (DPI) were 963 000 and 2.6 determined by GPC by using polystyrene standards. The sample was then alkaline-hydrolyzed for single-crystal preparation. The M_w and DPI after alkaline hydrolysis were 96 000 and 2.1, respectively.

Preparation of Single Crystals. The single crystals were grown in ethanol by an isothermal crystallization, according to the method reported previously.[17] P(4HB) (M_w = 96 000 and DPI = 2.1) was dissolved in ethanol at 140 °C for 30 min and then crystallized at 80 °C for 16 h to grow single crystals. Slow cooling was applied by cutting off the heating element in a silicone oil bath. The crystals were collected and washed by successive centrifugations with methanol at room temperature.

Transmission Electron Microscopy. Drops of the crystal suspension were deposited on carbon-coated grids, allowed to dry, and then shadowed with Pt−Pd alloy. For electron diffraction purposes, the crystals were only allowed to dry. Calibration of the patterns was done at room temperature, after depositing the crystals on gold-coated grids. The decoration of single crystals with polyethylene was performed by evaporating polyethylene on the crystals under a vacuum according to the method of Wittmann and Lotz[40] and then shadowed with Pt−Pd alloy. These grids were observed with a JEM-2000FX II electron microscope operated at an acceleration voltage of 120 kV for both electron diffraction and imaging of shadowed crystals. Electron diffraction diagrams and images were recorded on Fuji imaging plates and Mitsubishi MEM films. The observed intensities (I_{obs}) of electron reflections recorded on imaging plates were measured by using R-axis display software (Rigaku). The observed structure factor (F_{obs}) was taken as the square root of the corresponding intensities.

X-ray Diffraction Diagrams. X-ray fiber diffraction was performed on P(4HB) (M_w = 963 000 and DPI = 2.6) cast film that had been stretched to 550% followed by annealing at 55 °C for 7 days to increase the crystallinity.[17] A Rigaku-UltraX18-Rint X-ray generator operating at 40 kV and 200 mA was used in this study. An X-ray beam of Cu Kα of wavelength 0.1542 nm was used under evacuated conditions

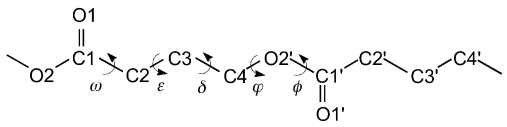

Figure 1. Definition of atom types and torsion angles in the dimer of P(4HB), used as the basic unit in the computed unit cells.

and calcium fluoride (d_{111} = 0.3154 nm) was used for calibration. The intensities of X-ray diffraction were measured with a Joyce-Loebl 3CS recording microdensitometer by scanning the same X-ray fiber diagram on which the observed *d*-spacings were measured. The layer tracings were resolved into individual integrated intensities by using a least-squares curve resolution program (Sarko, Computer program LSQ[41]). X-ray diffraction intensities were corrected in the usual way for multiplicity, Lorentz and polarization factors, arcing of diffractions, unequal film-to-sample distances of diffracted rays, and tracing directions other than radial and were then converted into relative structure factor amplitudes (Sarko, Computer program FIBRXRAY[42]).

Density Measurement. Densities of the P(4HB) stretched and annealed films, which were produced by the method described above for the X-ray diffraction diagram, were measured at 25 °C by flotation using aqueous NaBr solutions of increasing concentration.

Nomenclature. A representation of the atomic labeling scheme is shown in Figure 1. The conformation of the P(4HB) molecular chain is described by five torsion angles: ω = O2−C1−C2−C3, ϵ = C1−C2−C3−C4, δ = C2−C3−C4−O2′, φ = C3−C4−O2′−C1′, ϕ = C4−O2′−C1′−C2′.

Molecular Building and Packing Analysis. The software package Cerius[2] version 4.2 (Accelrys, Inc., USA) was used in the structural modeling, energy calculation, and diffraction simulation. The basic strategy was to determine the molecular conformation of the P(4HB) chain and the molecular packing arrangement within the experimental unit cell. After the initial model-building stage, a combination of energy minimization with the polymer consistent force field (PCFF) and simulations of diffraction patterns was used. In the computer-simulated X-ray diffraction patterns, the degrees of arcing and relative intensity were chosen to match the experimental X-ray diffraction pattern as closely as possible.

Enzymatic Degradation with PHB Depolymerase and Lipase. The extracellular PHB depolymerase from *Pseudomonas stutzeri* YM1006 and lipase from *Pseudomonas* sp. were purified to electrophoretic homogeneity by the methods of Ohura et al.[43] and Iwata et al.,[44] respectively. The enzymatic degradation of the P(4HB) films was carried out at 37 °C in Tris−HCl buffer (pH 7.5) with shaking at 108 rpm. Sample films (1 × 1 cm) were placed in small glass bottles containing 1 mL of Tris−HCl buffer. The reaction was started by the addition of 10 μL of an aqueous solution of lipase (300 μg/mL). Sample films were periodically removed, washed with distilled water, and dried to constant weight in a vacuum, and then the weights of the films were measured.

Degradation of P(4HB) single crystals was monitored using a turbidimetric assay. A 4 μL sample of a 200 μg/mL solution of an extracellular PHB depolymerase from *P. stutzeri* YM1006 or a 300 μg/mL solution of lipase from *Pseudomonas* sp. was added to 1 mL of 50 mM Tris−HCl buffer (pH 7.5) containing 0.4 mg/mL P(4HB) single crystals in a transparent plastic cuvette and then incubated at 37 °C. The turbidity at 660 nm (mOD_{660}) was measured during the enzymatic hydrolysis up to 90 min.

For transmission electron microscopy and atomic force microscopy study, the suspension of P(4HB) single crystals was dropped onto carbon-coated copper grids and silicon wafers, respectively. The grids and silicon wafers with attached single crystals were placed in a sterilized plastic cuvette containing 1 mL of buffer solution. The degradation was carried out in the same condition as that for turbidimetric assay. After degradation, the single crystals on grids or silicon wafers were carefully washed with Milli-Q water and dried in a vacuum.

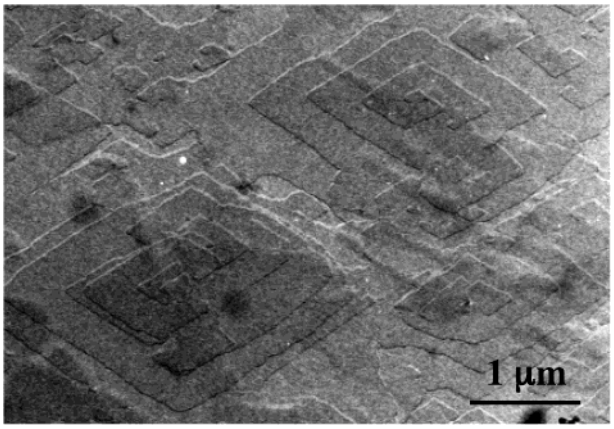

Figure 2. Electron micrograph of lozenge-shaped P(4HB) chain-folded lamellar crystals grown from ethanol, shadowed with Pt−Pd alloy.

Atomic Force Microscopy. The thicknesses and surface morphology of single crystals, before and after enzymatic degradation, were investigated by using AFM. AFM was performed with a SPI3700/SPA300 (Seiko Instruments Inc.). Pyramid-like Si_3N_4 tips, mounted on 100 μm long microcantilevers with spring constants of 0.09 N/m, were applied for the contact mode experiments. Simultaneous registration was performed in the contact mode for height and deflection images. Drops of the crystal suspension, before and after alkaline hydrolysis, were deposited on mica and allowed to dry. All images were recorded at room temperature.

Scanning Electron Microscopy. The surface morphologies of enzymatically degraded P(4HB) films were observed with a JSM-6330F scanning electron microscope after gold coating of the sample films using a SC-701 quick coater.

Molecular Weight Measurement. Molecular weights of all P(4HB) single crystals before and after enzymatic degradation were obtained by GPC at 40 °C, using a Shimadzu 10A GPC system and 6A refractive index detector with joint columns of Shodex K-80M and K-802 (each 4.6 × 300 mm). Chloroform was used as an eluent at a flow rate of 0.8 mL/min, and a sample concentration of 1.0 mg/mL was employed. The number-average and weight-average molecular weights (M_n and M_w) were calculated by using a Shimadzu Chromatopac C-R7A plus equipped with a GPC program. Polystyrene standards with a low polydispersity (Shodex Standard SM-105, 1.3×10^3 to 3.1×10^6) were used to generate a calibration curve.

Results and Discussion

Lamellar Single Crystals. Figure 2 shows P(4HB) lamellar single crystals grown in ethanol by an isothermal crystallization. They appear as lozenge-shaped crystals with screw dislocation, and the ratio between the two diagonal axes of the lozenge-shaped crystals was about 3:5. The crystals, which consist of stacks of lamellae, have various thicknesses: some are transparent to the electron beam, whereas others are completely opaque. Each monolamellar part at the edge of all P(4HB) single crystals yields a well-resolved electron diffraction diagram, and all electron diffraction diagrams are identical. Figure 3 shows the selected-area diffraction diagram of the lozenge-shaped lamellar crystals. The diffraction contains 14 independent diffraction spots mirrored in the four quadrants, defined by the two orthogonal axes a^* and b^*. Along these axes, systematic absences occurred at every odd reflection, which suggests that the diagram correspond to p2gg symmetry.

Figure 4 shows the P(4HB) lozenge-shaped lamellar crystals decorated with polyethylene. The polyethylene

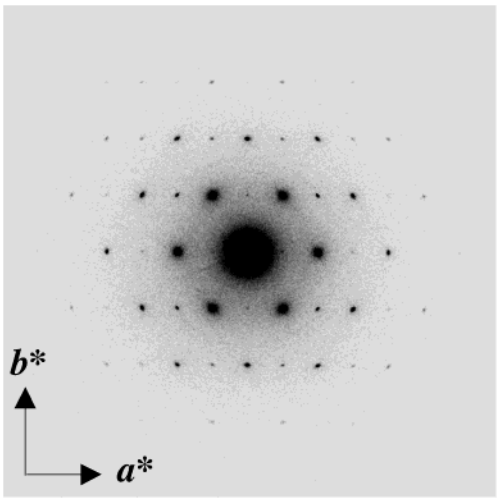

Figure 3. Electron diffraction diagram of a P(4HB) single crystal.

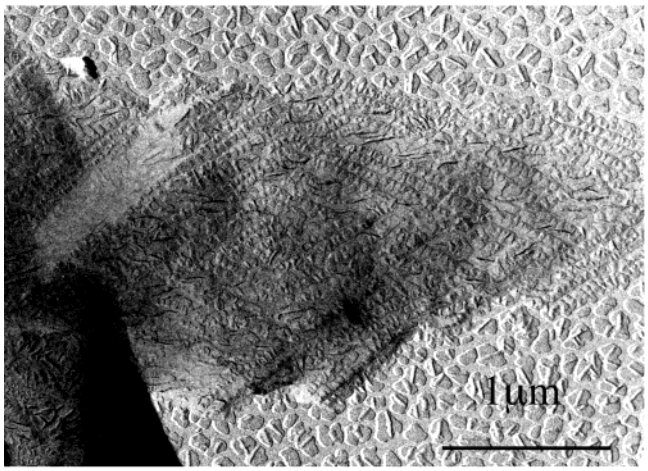

Figure 4. Typical electron micrograph of P(4HB) single crystals decorated with polyethylene and shadowed with Pt−Pd alloy.

rods are relatively well-ordered at the edges. The thickness by AFM of the monolamellar part of the lozenge-shaped crystals yielded the value of 8 nm. Taking the length of the all-trans conformation of P(4HB) molecules (1.240 nm[15]) and molecular weight into consideration, the molecular chains of P(4HB) must be folded within the lamella. Resulting from the triple exposure of the selected-area electron diffraction diagram and the normal and selected-area images, it was confirmed that the average chain-folding direction of P(4HB) corresponds to {110} planes.

Determination of Space Group and Unit Cell. The unit cell parameters and space group were determined through the electron diffraction pattern shown in Figure 3 and X-ray diffraction fiber diagrams shown in Figure 5. In Figure 5A, an arc reflection on the fifth meridian layer of the X-ray fiber diagram was observed. The fiber repeat distance of 0.232 nm calculated from this arc reflection on the meridian was not consistent with the values obtained from other layer reflections, suggesting that this is not a real reflection on the meridian. When the film was slightly tilted against the X-ray beam, this meridian reflection was split into two reflections as shown in Figure 5B. The observed (002) and (004) reflections of the tilted fiber diagram indicate that the chain conformation of P(4HB) is indeed a 2_1

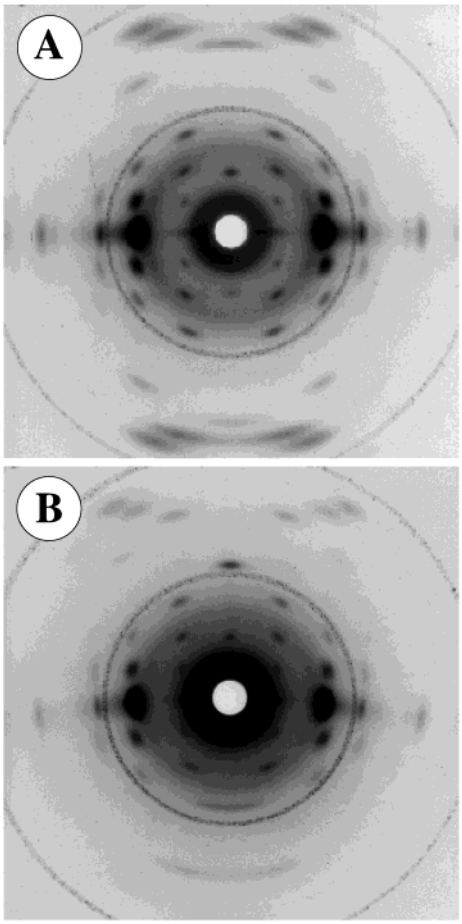

Figure 5. X-ray fiber diagrams of P(4HB) films: (A) 550% stretched and annealed at 55 °C for 7 days; (B) tilted diagram of (A), with a tilt angle of ca. 15°. The Debye−Scherrer ring of CaF_2 was used for calibration purposes.

helix. All the equatorial reflections of the X-ray fiber diagram are observed in the electron diffraction pattern, which confirms that the electron diffraction pattern is a projection along the *c*-axis, that is, the polymer chains are aligned perpendicular to the lamellar base of the crystal. Since the X-ray fiber diagram presents only even diffraction lines along the fiber axis and the electron diffraction pattern is consistent with p2gg symmetry, it can be concluded that P(4HB) crystals have the orthorhombic $P2_12_12_1$ space group, as reported previously.[13−17]

On the basis of the careful measurements of X-ray and electron diffraction patterns, the unit cell dimensions were calculated by a least-squares procedure. The X-ray diffraction diagram has a lower resolution than the electron diffraction diagram that displays diffraction spots down to 0.128 nm spacing as opposed to only 0.203 nm for the X-ray fiber diagram. P(4HB) crystallizes as an orthorhombic form with a $P2_12_12_1$ space group and lattice constants of $a = 0.775 \pm 0.002$ nm, $b = 0.477 \pm 0.002$ nm, and $c = 1.199 \pm 0.002$ nm. The calculated density for this unit cell is 1.29 g/cm^3, which is fairly close to the observed density of 1.22 g/cm^3. There are two chains in one unit cell, packed in an antiparallel arrangement, where each chain contains two residues. A comparison of the observed and calculated *d*-spacings in the electron diffraction diagram and X-ray fiber diagram is shown in Tables 1 and 2, respectively.

Molecular Conformation of the P(4HB) Chain. An all-trans, fully extended P(4HB) chain with a two-residue unit would be 1.240 nm, as reported by Pazur et al.[15] The P(4HB) crystal with a fiber repeat of 1.199 nm does not involve the fully extended chain; therefore, the molecule is slightly twisted in the unit cell. Usually, the conformation of the molecular chain is determined on the basis of energy calculation, such as in the case of poly([*R*]-3-hydroxybutyrate).[20,21,45,46] However, since there are five torsion angles in a P(4HB) chain as shown in Figure 1, the amount of calculation is too large to realize. In this work, conformational analysis has been performed based on energy minimization by using the Cerius^2 software.

Conformational studies of isotactic polylactone,[47] polypivalolactone,[48] and some other aliphatic polyesters[49] have been carried out by using energy minimization. Two approaches, that is, free-chain and bulk minimization, are often used in the determination of molecular conformation. In the former case, molecular conformation of the polymer chain is first built and then minimized while taking into account only the intramolecular (bonded and nonbonded) energy contribution. In the latter case, the minimization is carried out for a

Table 1. Crystallographic Data for P(4HB) Deduced from Electron Diffraction of Single Crystals

$hk0$[a]	d_{obs} (nm)	d_{calc} (nm)	$\|F_{obs}\|$[b]	$\|F_{calc}\|$
110	0.408	0.406	20.89	19.03
200	0.385	0.387	19.85	19.98
210	0.299	0.301	4.28	8.28
020	0.238	0.238	6.40	6.42
120	0.229	0.228	2.23	2.55
310	0.225	0.227	6.73	7.74
220	0.204	0.203	5.07	5.20
400	0.192	0.194	4.73	2.14
410	0.178	0.179	1.08	2.59
320	0.175	0.175	1.40	1.86
420	0.150	0.150	1.74	2.80
510	0.145	0.147	1.62	1.61
330	0.137	0.135	0.86	0.87
600	0.128	0.125	0.87	0.85

[a] Indexed in terms of an orthorhombic unit cell with parameters $a = 0.775$ nm, $b = 0.477$ nm, and c (fiber axis) $= 1.199$ nm. [b] $F_{obs} = (I_{obs})^{1/2}$, $\Sigma I_{obs} = \Sigma I_{calc} = 1000$.

Table 2. Crystallographic Data for P(4HB) Deduced from the X-ray Fiber Diagram of Stretched and Annealed Film

hkl[a]	d_{obs} (nm)	d_{calc} (nm)	$\|F_{obs}\|$[b]	$\|F_{calc}\|$[b]
110	0.410	0.406	7.69	8.18
200	0.382	0.387	7.64	9.02
210	0.300	0.301	4.76	4.16
020	0.239	0.238	2.52	3.02
120	0.227	0.228	6.14	4.86
310		0.227		1.59
220	0.203	0.203	7.37	3.88
400		0.194		1.67
101	0.648	0.651	0.98	1.02
011	0.444	0.443	0.92	3.13
111	0.386	0.385	6.18	5.78
201	0.367	0.369		
211	0.291	0.292	3.30	2.16
102	0.477	0.474	1.56	1.86
012	0.372	0.373	0.52	1.37
112	0.334	0.336	2.65	2.13
212	0.269	0.269	1.51	1.08
103	0.353	0.355	2.16	0.88
113	0.284	0.285	1.08	1.35
104	0.280	0.279	0.48	1.27
204	0.240	0.237	3.72	2.77
214	0.212	0.212	2.75	2.72

[a] Indexed in terms of an orthorhombic unit cell with parameters $a = 0.775$ nm, $b = 0.477$ nm, and c (fiber axis) $= 1.199$ nm. [b] $\Sigma F_{obs} = \Sigma F_{calc}$.

Table 3. Bond Lengths, Bond Angles, and Torsion Angles of the P(4HB) Molecular Chain

Bond Lengths (nm)			
C1−O1	0.120	C2−C3	0.154
C1−O2	0.134	C3−C4	0.152
C1−C2	0.152	C4−O2	0.142
Bond Angles (deg)			
O1−C1−O2	111.1	C2−C3−C4	116.4
O1−C1−C2	123.3	C3−C4−O2	104.9
C1−C2−C3	110.3	C4−O2−C1	120.8
Torsion Angles (deg)			
O2−C1−C2−C3	−173.4	C3−C4−O2′−C1′	163.6
C1−C2−C3−C4	178.6	C4−O2′−C1′−C2′	−175.1
C2−C3−C4−O2	−172.8		

polymer chain within a crystal taking into account both intra- and intermolecular interactions simultaneously. In this study, we use the bulk minimization method to determine the molecular conformation of P(4HB).

Since the fiber repeat of 1.199 nm is only 0.041 nm shorter than a fully extended chain of 1.240 nm,[15] it is reasonable to think that the torsion angles in the methylene sequences ω, ϵ, and δ are near to plane. Therefore, φ and ϕ, the torsion angles around the ester group, are regarded as variable parameters. In detail, the P(4HB) conformation with a fiber repeat of 1.199 nm and a 2_1 screw symmetry along the chain axis was determined as follows:

(1) A residue of P(4HB) was built by using the structure-builder of Cerius[2].

(2) ω, ϵ, and δ of the residue were set from 160° to 200° in an increment of 10°, so there were 125 starting states.

(3) The residue with certain ω, ϵ, and δ was then put into a unit cell with the experimental lattice parameters, and the chain axis of the residue was set in coincidence with one of the 2_1 crystallographic axes parallel to the *c* axis.

(4) The other three residues were then constituted according to the symmetry of $P2_12_12_1$.

(5) Two residues were connected to form one molecular chain.

(6) Energy minimization was carried out for the molecular conformations within the unit cell. The unit cell parameter, including the fiber repeat of 1.199 nm, and the space group were constrained during the minimization process.

All of the 125 conformers reached the same conformation after minimization, so this conformation is regarded as the reliable conformation and is used in the structure refinement. The bond lengths, bond angles, and torsion angles are listed in Table 3. The conformation of the chain is characterized by torsion angles $\omega = -173.4°$, $\epsilon = 178.6°$, $\delta = -172.8°$, $\varphi = 163.6°$, and $\phi = -175.1°$.

Structure Refinement. Packing of polymer chains in the crystal including setting angle orientations and the relative shift of molecules in the unit cell are often studied taking into account both experimental diffraction data and energy calculation.[50,51] A reliability factor (*R*-factor) study was carried out in order to determine the most favorable setting angle. For this purpose, the setting angle, θ, with respect to the *b* axis, was varied from 0° to 180° in steps of 10° and the *R*-factor and energy were evaluated. Figure 6 shows the *R*-factor against electron diffraction data and energy as a function of the setting angle θ with respect to the *b* axis. The most favorable arrangement corresponds to $\theta = 30°$ and 120° as for the *R*-factor; in the meanwhile, the energy at $\theta = 30°$ is lower than 120°. Accordingly, the *R*-factor and setting angle map was recomputed using finer grid steps, 1°, from 25° to 35°. The results showed that the most favorable arrangement was 29° with respect to the *b* axis. The rotation angles between the plane of the polymer chain and the *a* axis are 51.5° for PPL[8] and 58° for PVL.[9] The setting angle of P(4HB) around the molecular axis determined in this study is 61°. Recently, the crystal structure of poly(ω-pentadecalactone) was determined by Gazzano et al.,[52] and they reported that the backbone conformation is all-trans and the setting angle, with respect to the *a* axis, is 48°. The stable position of molecular chains with the all-trans conformation around the molecular axis seems to be almost the same.

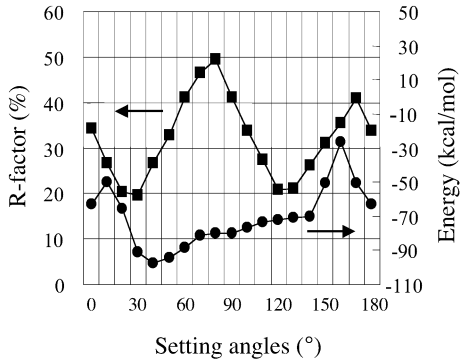

Figure 6. Reliability factors (*R*-factors) and energy as a function of the setting angles with respect to the *b* axis. The observed intensities of the electron diffraction diagram as listed in Table 1 were used to calculate the *R*-factor.

Table 4. Fractional Atomic Coordinates of P(4HB)

atom	*x*	*y*	*z*
C1	+0.2914	+0.0982	+0.4271
C2	+0.2029	−0.0805	+0.3388
C3	+0.2312	+0.0464	+0.2223
C4	+0.1535	−0.1141	+0.1246
O1	+0.3630	+0.3180	+0.4106
O2	+0.2836	−0.0253	+0.5278

The translation along the molecular axis was carried out against X-ray diffraction intensity data. The shift parameter along the molecular axis was changed from 0 to 0.5*c* (*c* = 1.199 nm) at the rate of 0.01*c*. Since the unit cell has three sets of 2-fold screw symmetry axes and two antiparallel chains exist in it, this translation of up to 0.5*c* covers all translation positions. The optimized shift value along the molecular axis is 0.1*c*. In this position, all of the parameters and torsion angles were further refined. A final model was obtained which yielded $R = 0.223$ with X-ray diffraction data and $R = 0.176$ with electron diffraction data. The lists of observed and calculated structure factors with the final model are presented in Tables 1 and 2 for electron and X-ray diffraction data, respectively. The list of the fractional coordinates is presented in Table 4, and the packing of the chain in the crystal is shown in projection in Figure 7. One sees that the {110} growth planes of the crystal are indeed parallel to the direction of the highest atomic densities, as expected.

Enzymatic Degradation of P(4HB) Films with Lipase from *Pseudomonas* sp. Three types of P(4HB) films, solution-cast film, stretched film, and stretched−annealed film, were used for enzymatic degradation tests with lipase from *Pseudomonas* sp. The enzymatic degradation of P(4HB) films was carried out in Tris−

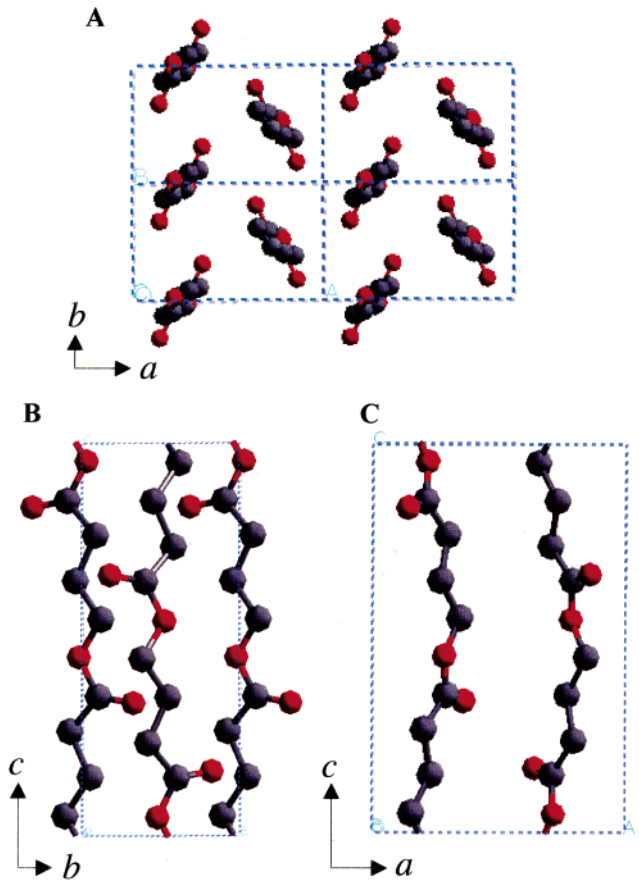

Figure 7. (A) Projection of the P(4HB) structure in the *ab* plane, (B) projection of the P(4HB) structure in the *bc* plane, and (C) projection of the P(4HB) structure in the *ac* plane. Hydrogen atoms are omitted.

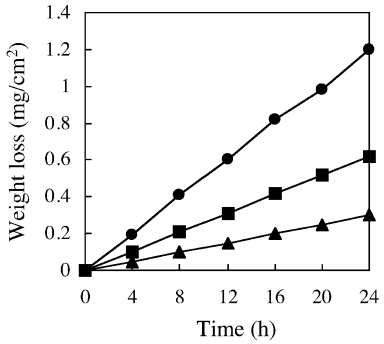

Figure 8. Enzymatic degradation of P(4HB) films in an aqueous solution of lipase from *Pseudomonas* sp. at 37 °C: (●) solution-cast, (■) stretched, and (▲) stretched−annealed film.

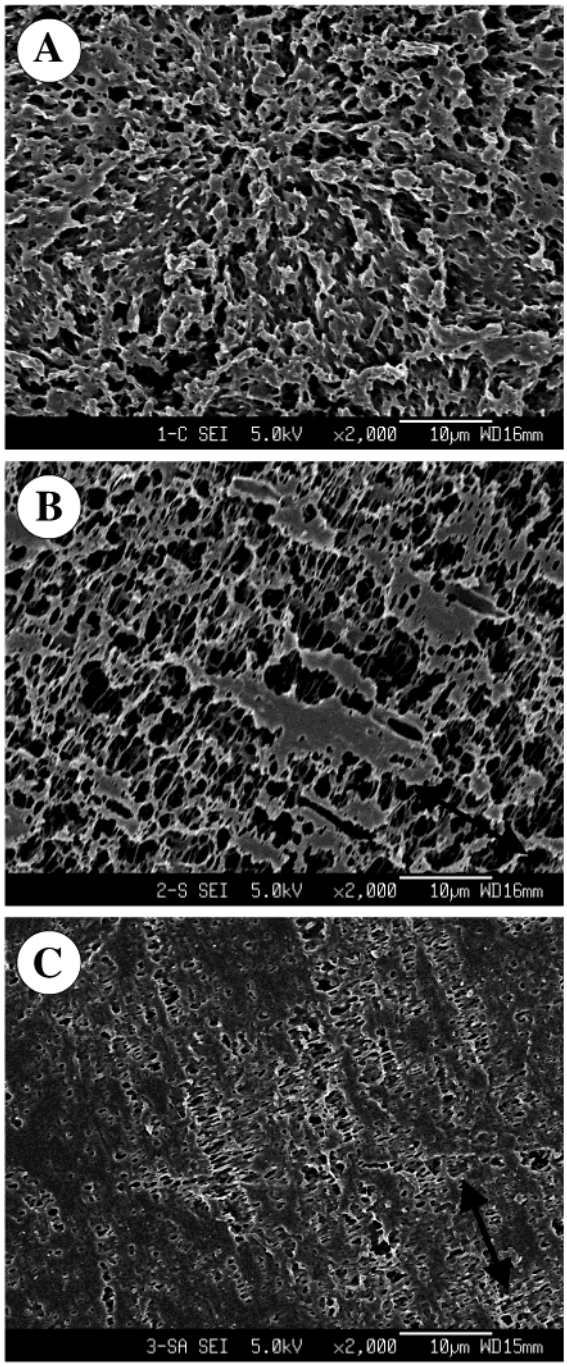

Figure 9. Scanning electron micrographs of P(4HB) films after partial enzymatic degradation by lipase from *Pseudomonas* sp.: (A) solution-cast, (B) stretched, and (C) stretched−annealed film.

HCl buffer solution containing lipase from *Pseudomonas* sp. at 37 °C and pH 7.5. Figure 8 shows typical weight-loss profiles of P(4HB) films during the enzymatic degradation. The weight losses of films increased proportionally with time. The rate of enzymatic degradation could be determined from the slope of the weight loss against time, and the degradation rates were in the order of solution-cast film > stretched film > stretched−annealed films. It is obvious that the rate of enzymatic degradation decreases markedly with an increase in crystallinity.

Figure 9 shows the scanning electron micrographs of the solution-cast, stretched, and stretched−annealed films after partial degradation with lipase from *Pseudomonas* sp. for 24 h at 37 °C. Before enzymatic hydrolysis and after treatment in buffer solution without lipase, the surfaces of the P(4HB) films were flat. However, after enzymatic degradation, the morphologies of the surfaces changed greatly. Spherulites could be observed on the surface of the solution-cast film as shown in Figure 9A. In Figure 9B,C, shish-kebab morphologies were observed on the surfaces of enzymatically degraded stretched and stretched−annealed films. These results indicate that the amorphous regions on the film surfaces were first eroded and then crystal regions were cropped out. A larger part of the stretched−annealed film remained flat in Figure 9C compared to that in Figure 9A,B, further proving the rate of enzy-

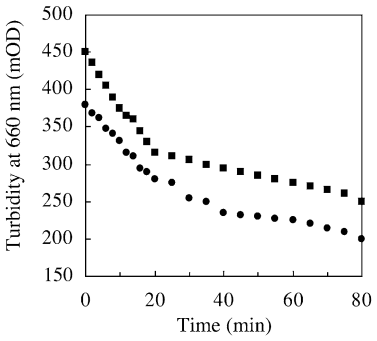

Figure 10. Decrease in turbidity versus time during the enzymatic degradation of P(4HB) single crystals with (●) extracellular PHB depolymerase from *P. stutzeri* YM1006 and (■) lipase from *Pseudomonas* sp.

matic degradation decreases with an increase in crystallinity.

Shish-kebab morphologies were also observed in stretched and stretched−annealed films of ultrahigh-molecular-weight P(3HB) after degradation using extracellular PHB depolymerase.[53] P(4HB) films showed similar degradation phenomena as P(3HB) films revealed by the rate of erosion profiles and SEM observations. The solution-cast films of both of P(3HB) and P(4HB) have more amorphous region and are etched faster than the stretched and stretched−annealed films. In stretched and stretched−annealed films, amorphous regions are etched first. As a result, the unetched core along the draw direction and lamellar crystals perpendicular to the core, shish-kebab morphologies, are observed in SEM micrographs.

Enzymatic Degradation of P(4HB) Single Crystals with Lipase from *Pseudomonas* sp. and PHB Depolymerase from *P. stutzeri* YM1006. Since the direct observation of the morphological changes of the lamellar crystals is profitable for elucidation of the degradation mechanism in the crystal region, the preparation and degradation of single crystals of biodegradable polymers have been carried out by the research groups of Marchessault,[28−30,54,55] Chanzy,[54] and Iwata.[31,32,56−58] Besides P(3HB),[28−32,56−58] the degradation mechanisms of xylan,[54] nigeran,[55] P(3HB) copolymers,[59,60] PPL,[61] poly(ethylene succinate) (PES),[62] poly(L-lactic acid) (PLLA),[63] and PCL[44] have also been investigated.

In this work, enzymatic degradation of P(4HB) single crystals was carried out in Tris−HCl buffer solution containing lipase from *Pseudomonas* sp. and an extracellular PHB depolymerase from *P. stutzeri* YM1006, respectively. The degradation of P(4HB) single crystals by PHB depolymerase or lipase was monitored using a turbidity assay as shown in Figure 10. The turbidities decreased fast in the beginning 20 min and after that decreased slowly, which seem to correspond to the degradations of the loosely chain-packed regions and of the tightly chain-packed regions in the crystal.

Images A and B in Figure 11 show the electron micrographs of P(4HB) single crystals degraded with lipase from *Pseudomonas* sp. and with PHB depolymerase from *P. stutzeri* YM1006 for 30 min at 37 °C, respectively. While P(4HB) yielded lozenge-shaped multilamellar crystals with smooth edges before treatment (Figure 2), after partial enzymatic degradation, edges of the crystal became rough; however, the surface of the crystal was still plane and clean. The thickness of P(4HB) single crystals, before and after enzymatic

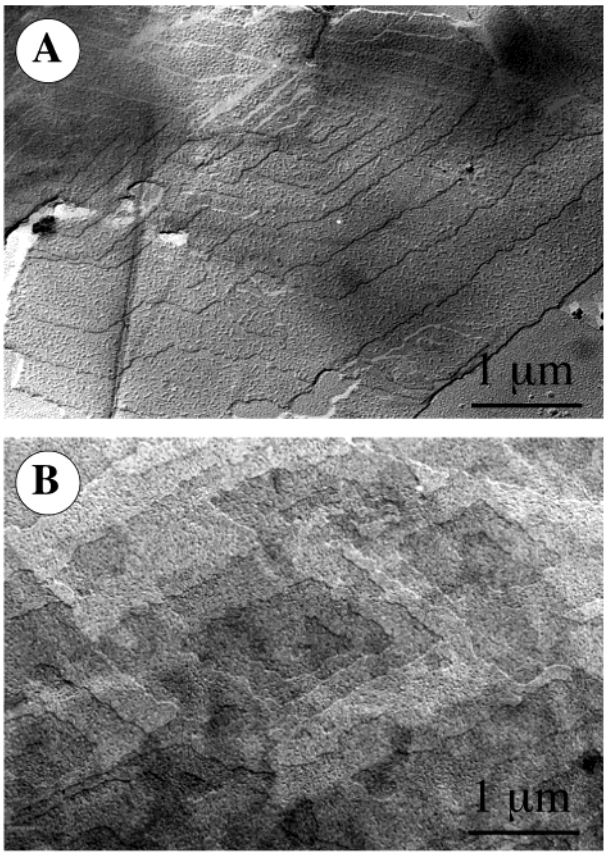

Figure 11. Electron micrographs of P(4HB) single crystals after partial enzymatic degradation for 30 min with (A) lipase from *Pseudomonas* sp. and (B) extracellular PHB depolymerase from *P. stutzeri* YM1006.

degradation, was investigated by AFM. The multilamellar crystal has a flat surface, and every layer has a height of about 8 nm before degradation. On the basis of the lamellar thickness, the fiber repeat distance and the molecular weights, it is confirmed that the molecular chains of P(4HB) are folded within the lamella as described in the section Lamellar Single Crystals. The thickness of the crystals remained unchanged after partial enzymatic degradation as shown in Figure 12, suggesting that the chain-folding regions on the crystal surface are not degraded by the action of enzyme molecules. The molecular weights of P(4HB) single crystals before and after enzymatic degradation also remained unchanged (data not shown). Taking account of morphological changes and the lack of decrease in molecular weight and lamellar thickness, it can be concluded that enzymatic degradation takes place from the crystal edges rather than the chain-folding surface. In our previous research for PPL[8] and PVL[9] chain-folding conformations on the crystal surface, it was revealed that the molecular conformation with all-trans in the crystalline core changed to gauche and kink conformations in the adjacent chain-folding region. These conformational differences should be one of the reasons that enzyme molecules cannot attack the chain-folding region.

In the case of P(3HB) and PPL, which have chemical structures similar to that of P(4HB), enzymatic degradation also commenced from the edges of the single crystals. However, the morphologies after enzymatic degradation are different. Lath-shaped P(3HB) lamellar crystals are degraded from the edges and along their long axis yielding lathlike fingers and crystal frag-

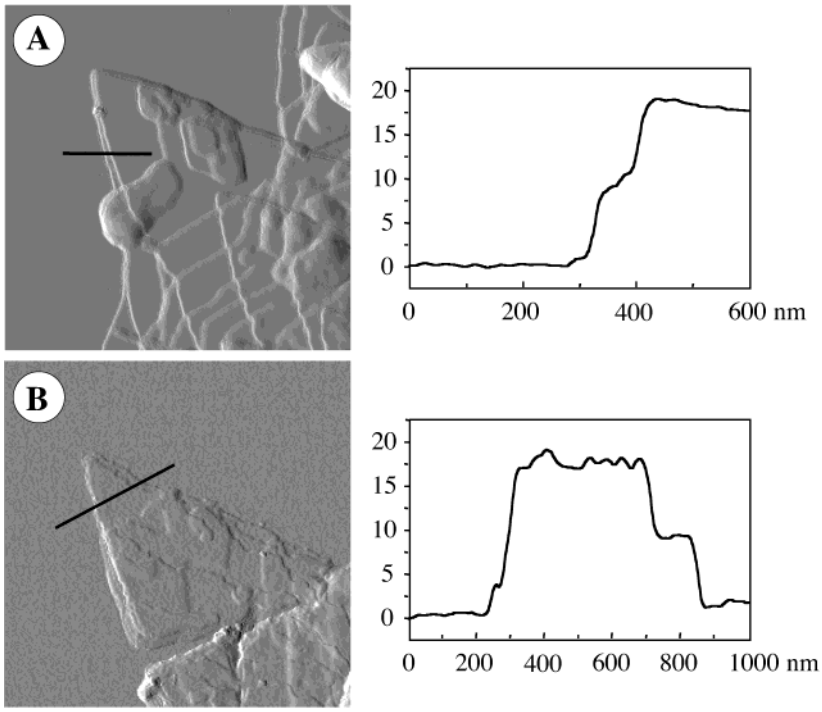

Figure 12. AFM images of P(4HB) single crystals and line profile data: (A) before and (B) after enzymatic degradation by an extracellular PHB depolymerase purified from *P. stutzeri* YM1006.

ments.[30−32,56,57] Lath-shaped PPL[61] and lozenge-shaped P(4HB) lamellar crystals are only degraded from the crystal edges without yielding cracks and crystal fragments. The different degradation behavior between P(3HB) with PPL and P(4HB) may be due to the difference in crystal stability. The molecular conformation in P(3HB) is a 2_1 helix, while the molecular conformation in PPL single crystals is all-trans. Though the molecular conformation of P(4HB) is a 2_1 helix, in fact, it is near all-trans. Therefore, P(3HB) molecular chains are packed loosely and sometimes improperly in lamellar crystals compare to PPL and P(4HB), so the enzymes attack the P(3HB) crystals more easily. Accordingly, degradation progressed only from the crystal edges without yielding narrow cracks and crystal fragments for PPL and P(4HB).

Conclusions

The molecular and crystal structure of P(4HB) has been determined utilizing intensities measured from X-ray fiber diffraction data and electron diffraction data of single crystals combined with energy minimization. The lozenge-shaped P(4HB) single crystals have the average chain-folding direction of $\{11\bar{0}\}$ planes with alternation in the diagonal (110) and $(1\bar{1}0)$ planes. The P(4HB) crystal has an orthorhombic $P2_12_12_1$ space group with cell parameters $a = 0.775 \pm 0.002$ nm, $b = 0.477 \pm 0.002$ nm, and c (fiber axis) $= 1.199 \pm 0.002$ nm. Density considerations lead to two chains per unit cell, which exist in an antiparallel arrangement. The helical conformation is characterized as near all-trans. The setting angles, with respect to the b axis, are $\pm 29°$ for the corner and center chains. By using the electron and X-ray diffraction data, the best molecular packing model was refined to R-factors of 0.176 and 0.223, respectively.

The rate of enzymatic erosion of P(4HB) films, solution-cast, stretched, and stretched−annealed films, decreased with an increase in the degree of crystallinity by lipase from *Pseudomonas* sp. Shish-kebab structure was observed inside the stretched films after partial enzymatic degradation. Lozenge-shaped single crystals of P(4HB) were partially degraded by both lipase and extracellular PHB depolymerase from *P. stutzeri* YM1006 to yield crystals with notched edges. The lamellar thickness and molecular weight of the crystals remained unchanged, indicating that enzymatic degradation does not progress at the chain-folding region on the crystal surface. P(4HB) has near all-trans conformation in the crystal core; however, the adjacent reentry chain-folding seems to occur on the crystal surface with gauche or kink conformations. These conformational differences should be hindered by the action of the catalytic domain in enzyme molecules.

Acknowledgment. This research was supported by the grant for Ecomolecular Science Research at the RIKEN Institute and a Grant-in-Aid for Young Scientists (A) No.15685009 (2003) from the Ministry of Education, Culture, Sports, Science and Technology, Japan.

References and Notes

(1) Doi, Y. *Microbial Polyesters*; VCH: New York, 1990.
(2) Sudesh, K.; Fukui, T.; Taguchi, K.; Iwata, T.; Doi, Y. *Int. J. Biol. Macromol.* **1999**, *25*, 79.
(3) Hein, S.; Sohling, B.; Gottschalk, G.; Steinbüchel, A. *FEMS Microbiol. Lett.* **2000**, *153*, 411.
(4) Saito, Y.; Doi, Y. *Int. J. Biol. Macromol.* **1994**, *16*, 99.
(5) Saito, Y.; Nakamura, S.; Hiramitsu, M.; Doi, Y. *Polym. Int.* **1996**, *39*, 169.
(6) Sodian, R.; Hoerstrup, S. P.; Sperling, J. S.; Martin, D. P.; Daebritz, S.; Mayer, J. E., Jr.; Vacanti, J. P. *ASAIO J.* **2000**, *46*, 107.
(7) Sudesh, K.; Abe, H.; Doi, Y. *Prog. Polym. Sci.* **2000**, *25*, 1503.
(8) Furuhashi, Y.; Iwata, T.; Sikorski, P.; Atkins, E.; Doi, Y. *Macromolecules* **2000**, *33*, 9423.
(9) Furuhashi, Y.; Sikorski, P.; Atkins, E.; Iwata, T.; Doi, Y. *J. Polym. Sci., Part B*: *Polym. Phys.* **2001**, *39*, 2622
(10) Chatani, Y.; Okita, Y.; Tadokoro, H.; Yamashita, Y. *Polym. J.* **1970**, *1*, 555.

(11) Bittiger, H.; Marchessault, R. H. *Acta Crystallogr.* **1970**, *B26*, 1923.
(12) Hu, H.; Dorset, D. L. *Macromolecules* **1990**, *23*, 4604.
(13) Mitomo, H.; Kobayashi, S.; Morishita, N.; Doi, Y. *Polym. Prepr., Jpn* **1995**, *44*, 3156.
(14) Kobayashi, S.; Kogure, K.; Mitomo, H.; Doi, Y. *Polym. Prepr., Jpn* **1998**, *47*, 968.
(15) Pazur, R. J.; Raymond, S.; Hocking, P. J.; Marchessault, R. H. *Polymer* **1998**, *39*, 3065.
(16) Nakamura, K.; Yoshie, N.; Sakurai, M.; Inoue, Y. *Polymer* **1994**, *35*, 193.
(17) Su, F.; Iwata, T.; Sudesh, K.; Doi, Y. *Polymer* **2001**, *42*, 8915.
(18) Lemoignei, M. *Ann. Inst. Pasteur* **1925**, *39*, 144.
(19) Lemoignei, M. *Ann. Inst. Pasteur* **1927**, *41*, 148.
(20) Okamura, K.; Marchessault, R. H. *Conformation of Biopolymers*; Ramachandran, G. N., Ed.; Academic Press: New York, 1967; Vol. 2, p 709.
(21) Yokouchi, M.; Chatani, Y.; Tadokoro, H.; Teranishi, K.; Tani, H. *Polymer* **1973**, *14*, 267.
(22) Lundgren, D. G.; Alper, R.; Schnaitman, C.; Marchessault, R. H. *J. Bacteriol.* **1965**, *89*, 245.
(23) Marchessault, R. H.; Coulombe, S.; Morikawa, H.; Okamura, K.; Revol, J.-F. *Can. J. Chem.* **1981**, *59*, 38.
(24) Doi, Y.; Kitamura, S.; Abe, H. *Macromolecules* **1995**, *28*, 4822.
(25) Tomasi, G.; Scandola, M.; Briese, B. H.; Jendrossek, D. *Macromolecules* **1996**, *29*, 507.
(26) Koyama, N.; Doi, Y. *Macromolecules* **1997**, *30*, 826.
(27) Abe, H.; Kikkawa, Y.; Iwata, T.; Aoki, H.; Akehata, T.; Doi, Y. *Polymer* **2000**, *41*, 867.
(28) Hocking, P. J.; Revol, J.-F.; Marchessault, R. H. *Macromolecules* **1996**, *29*, 2467.
(29) Hocking, P. J.; Marchessault, R. H.; Timmins, M. R.; Lenz, R. W.; Fuller, R. C. *Macromolecules* **1996**, *29*, 2472.
(30) Nobes, G. A. R.; Marchessault, R. H.; Chanzy, H.; Briese, B. H.; Jendrossek, D. *Macromolecules* **1996**, *29*, 2472.
(31) Iwata, T.; Doi, Y.; Kasuya, K.; Inoue, Y. *Macromolecules* **1997**, *30*, 833.
(32) Iwata, T.; Doi, Y.; Tanaka, T.; Akehata, T.; Shiromo, M.; Teramachi, S. *Macromolecules* **1997**, *30*, 5290.
(33) Doi, Y.; Segawa, A.; Kunioka, M. *Int. J. Biol. Macromol.* **1990**, *12*, 106.
(34) Doi, Y.; Kanesawa, Y.; Kunioka, M.; Saito, T. *Macromolecules* **1990**, *23*, 26.
(35) Saito, Y.; Doi, Y. *Int. J. Biol. Macromol.* **1994**, *16*, 99.
(36) Saito, Y.; Nakamura, S.; Hiramitsu, M.; Doi, Y. *Polym. Int.* **1996**, *39*, 169.
(37) Sudesh, K.; Fukui, T.; Taguchi, K.; Iwata, T.; Doi, Y. *Int. J. Biol. Macromol.* **1999**, *25*, 79.
(38) Mukai, K.; Doi, Y.; Sema, Y.; Tomita, K. *Biotechnol. Lett.* **1993**, *15*, 601.
(39) Hein, S.; Sohling, B.; Gottschalk, G.; Steinbüchel, A. *FEMS Microbiol. Lett.* **2000**, *153*, 411.
(40) Wittmann, J. C.; Lotz, B. *J. Polym. Sci., Polym. Phys. Ed.* **1985**, *23*, 205.
(41) Sarko, A. *LSQ* (Fortran least-squares curve resolution program); College of Environmental Science and Forestry, SUNY: Syracuse, NY.
(42) Sarko, A. *FIBRXRAY* (Fortran X-ray intensity correction program); College of Environmental Science and Forestry, SUNY: Syracuse, NY.
(43) Ohura, T.; Kasuya, K.; Doi, Y. *Appl. Environ. Microbiol.* **1999**, *65*, 189.
(44) Iwata, T.; Doi, Y. *Polym. Int.* **2002**, *51*, 852.
(45) Cornibert, J.; Marchessault, R. H. *J. Mol. Biol.* **1972**, *71*, 735.
(46) Brückner, S.; Meille, S. V.; Malpezzi, L.; Cesàro, A.; Navarini, L.; Tombolini, R. *Macromolecules* **1988**, *21*, 967.
(47) He, Z.; Brisson, J.; Prud'homme, R. E. *Macromolecules* **1998**, *31*, 8209.
(48) Ferro, D. R.; Brückner, S.; Meille, S. V.; Ragazzi, M. *Macromolecules* **1990**, *23*, 1676.
(49) Liau, W. B.; Boyd, R. H. *Macromolecules* **1990**, *23*, 1531.
(50) Andre, I.; Mazeau, K.; Tvaroska, I.; Putaux, J.-L.; Winter, W. T.; Taravel, F. R.; Chanzy, H. *Macromolecules* **1996**, *29*, 4626.
(51) Alemán, C.; Lotz, B.; Puiggali, J. *Macromolecules* **2001**, *34*, 4795.
(52) Gazzano, M.; Malta, V.; Focarete, M. L.; Scandola, M.; Gross, R. A. *J. Polym. Sci., Part B: Polym. Phys.* **2003**, *41*, 1009.
(53) Kusaka, S.; Iwata, T.; Doi, Y. *Int. J. Biol. Macromol.* **1999**, *25*, 87.
(54) Chanzy, H.; Comtat, J.; Dube, M.; Marchessault, R. H. *Biopolymers* **1979**, *18*, 2459.
(55) Marchessault, R. H.; Revol, J. F.; Bobbitt, T. F.; Hordin, J. H. *Biopolymers* **1980**, *19*, 1069.
(56) Murase, T.; Iwata, T.; Doi, Y. *Macromolecules* **2001**, *34*, 5848.
(57) Murase, T.; Iwata, T.; Doi, Y. *Macromol. Biosci.* **2001**, *1*, 275.
(58) Iwata, T.; Doi, Y. *Macromol. Chem. Phys.* **1999**, *200*, 2429.
(59) Nobes, G. A. R.: Marchessault, R. H.; Breise, B. H.; Jendrossek, D. *J. Environ. Polym. Degrad.* **1998**, *6*, 99.
(60) Iwata, T.; Doi, Y.; Nakayama, S.; Sasatsuki, H.; Teramachi, S. *Int. J. Biol. Macromol.* **1999**, *25*, 169.
(61) Furuhashi, Y.; Iwata, T.; Doi, Y. *Sen'i Gakkaishi* **2001**, *57*, 184.
(62) Iwata, T.; Doi, Y.; Isono, K.; Yoshida, Y. *Macromolecules* **2001**, *34*, 7343.
(63) Iwata, T.; Doi, Y. *Macromolecules* **1998**, *31*, 2461.

MA034546S